Cardiovasc Res **1:** 11-17, 1971
6. Schilling MO: Capacitance transducer for muscle research. Rev Sci Instr **31:** 1215-1217, 1960
7. Steiger GJ: Stretch activation and tension transients in cardiac, skeletal and insect flight muscle. *In* Proceedings of Symposium on Insect Flight Muscles at Oxford, England, edited by RT Tregear, JWS Pringle. New York, North Holland, 1977, pp 221-268
8. Bozler E: Feedback in the contractile mechanism of the frog heart. J Gen Physiol **60:** 239-247, 1972
9. Bozler E, Delahayes JF: Mechanical and electrical oscillations in cardiac muscle of the turtle. J Gen Physiol **62:** 523-532, 1973
10. Henderson AH, Cattell MR: Length-induced changes in activation during contraction of cat and frog heart muscle. Circ Res **38:** 289-296, 1976
11. Gibbons WR, Fozzard HA: High potassium and low sodium contractures in sheep cardiac muscle J Gen Physiol **58:** 483-510, 1971
12. Slavicek J: Effect of Ba^{2+} contractility of the isolated right rat ventricle. Substitution of NaCl for choline or hypertonic sucrose. Physiol Bohemoslov **21:** 189-199, 1972
13. Sanborn WG, Langer GA: Effects of contractile activation of strontium and barium in the rabbit ventricle (abstr). Fed Proc **33:** 302, 1974
14. Mascher D: Electrical and mechanical responses in ventricular muscle fibres during barium perfusion Pfluegers Arch **342:** 325-346, 1973
15. Reuter H: Divalent cations as charge carriers in excitable membranes. Prog Biophys Mol Biol **26:** 1-43, 1973
16. Ebashi S, Endo M: Calcium ion and muscle contraction. Prog Biophys Mol Biol **18:** 123-183, 1968
17. Heinl P: Mechanische Aktivierung und Deaktivierung der isolierten-contractilen Strukter des Froschsartorius durch rechteckförmige und sinusformige Längenänderungen. Pfluegers Arch **333:** 213-226, 1972
18. Steiger GJ: Tension transients in extracted heart muscle preparations of rabbit. J Mol Cell Cardiol **9:** 671-685, 1977
19. Heinl P, Herzig J, Sawaya MCB, Steiger GJ: Myofibrilläre Rückkopplung von Längen- und Spannungsänderungen in isolierten kontraktilen Strukturen verschiedener Vertebratenherzmuskeln mit unterschiedlicher Schlagfrequenz (abstr). Pfluegers Arch **339:** 212, 1973
20. Bárány M, Gaetjens E, Bárány K, Karp E: Comparative studies of rabbit cardiac skeletal myosins Arch Biochem Biophys **106:** 280-293, 1964
21. White DCS, Thorson J: The kinetics of muscle contraction Prog Biophys Mol Biol **27:** 173-255, 1973
22. Schädler M, Steiger GJ, Rüegg JC: Mechanical activation and isometric oscillation in insect fibrillar muscle. Pfluegers Arch **330:** 217-229, 1971
23. Steiger GJ, Rüegg JC, Boldt KM, Lübbers DW, Breull W: Changes in the polarization of tryptophan fluorescence in the actomyosin system of working muscle fibres. Cold Spring Harbor Symp Quant Biol **37:** 377-378, 1972
24. Steiger GJ: Wirkungweise, Energetik und Nutzeffekt der isolierten kontraktilen Struktur Maschine fibriallarer Insektenflugmuskeln. Ph.D. Dissertation, Universitat Karlsruhe, 1969

The Electrocardiographic Recognition of Cardiac States at High Risk of Ventricular Arrhythmias

An Experimental Study in Dogs

PAUL M. URIE, MARY JO BURGESS, ROBERT L. LUX, ROLAND F. WYATT, AND J. A. ABILDSKOV

SUMMARY **Recognition of states in which the heart is vulnerable to arrhythmia would be a helpful guide to prophylaxis. The possibility of recognizing such states from the ECG is suggested by the already established relations between abnormally disparate recovery to both vulnerability to arrhythmia and ECG waveform. In this study, canine QRS, T, and QRST isoarea maps were determined from ECGs recorded at 192 body sites during control states and conditions of enhanced susceptibility to arrhythmia. Vulnerable states were produced by ouabain intoxication, hypothermia, premature beats, and epinephrine infusion. A hypothetical series of QRST isoarea maps that would be expected to occur without increased local inequalities of recovery was derived by adding the control QRS isoarea map to a fraction (α) of the control T isoarea map and allowing the fraction to vary from $\alpha = 1$ to $\alpha = -1$. One QRST isoarea map selected from the derived series was subtracted from a QRST isoarea map during each state of enhanced arrhythmia vulnerability. Derived maps were selected to minimize the average amplitude of the residual maps. RMS values of the residual maps systematically increased with increasing prematurity of depolarization, with time after a toxic injection of a dose of ouabain, with increasing hypothermia, and during the first 3 minutes of epinephrine infusion. Also, the RMS values of the residual maps decreased in hypothermic dogs during rewarming. Our findings suggest that states of vulnerability to arrhythmia due to increased disparity of recovery can be identified by analysis of ECG waveforms recorded from lead systems sensitive to electrical activity in local cardiac regions.**

A RELATIONSHIP between disparate recovery of excitability in cardiac muscle and vulnerability to arrhythmias has been established.[1-4] Inequalities of ventricular recovery also are responsible for the ST-T waveform in the electrocardiogram.[5] These relationships suggest that conditions associated with a high risk of ventricular arrhythmias might be evident from the ST-T deflection. We examined this possibility through experiments on dogs in which we used interventions known to enhance vulnerability to arrhythmia. Multiple body surface leads were used to detect the electrical state in local cardiac regions, since the relationship of recovery and arrhythmia vulnerability which has been demonstrated is that of disparate recovery in localized cardiac areas. A new method of analysis of the QRST deflection recorded from multiple leads was developed. In this analysis, the QRST area was

From the Nora Eccles Harrison Cardiovascular Research and Training Institute, and the Division of Cardiology, Department of Internal Medicine, University of Utah College of Medicine, Salt Lake City, Utah.

Supported, in part, by Program Project Grant HL 13480 from the National Institutes of Health, and the Richard A and Nora Eccles Harrison Fund for Electrocardiographic Research.

Address for reprints: Paul M. Urie, Ph.D., Cardiology Division, Building 100, University of Utah, Salt Lake City, Utah 84132.

Received April 25, 1977; accepted for publication October 4, 1977.

used as an index of disparate recovery to minimize the secondary influence of activation sequence on that of recovery.[6] In addition, we formulated an hypothesis that normal ventricular recovery properties could change without including abnormal disparity of recovery. The body surface distributions of QRST areas to be expected with such states of abnormal recovery, but without increased local disparity of recovery, were predicted and compared to those recorded during conditions of enhanced arrhythmia vulnerability. Our findings suggested a relationship between vulnerability to ventricular arrhythmia and electrocardiographic features detectable by this analysis. Since the analysis was designed to detect increased disparity of ventricular recovery, the results indirectly suggest that ECG findings were due to this feature of ventricular states with enhanced arrhythmia vulnerability.

Methods

Experiments were performed on 10 closed-chest dogs anesthetized with pentobarbital, 30 mg/kg, iv. Bipolar pacing catheters were placed in the right atrium, right ventricle, and left ventricle to maintain heart rate control and introduce premature stimuli. For the experiments in which ouabain and hypothermia were employed, ventricular stimuli were used to permit observations to be continued despite the appearance of slow atrioventricular (AV) conduction and AV dissociation. Premature beats also were initiated from ventricular sites. When the ventricular sites were driven, the atrial site was stimulated simultaneously to decrease the possibility of reentry and to keep constant the effects of atrial activation on ECG waveform. In all experiments, control and postintervention records were obtained at the same heart rate.

States of altered vulnerability to arrhythmia were produced by hypothermia, ouabain intoxication, premature beats, and epinephrine infusion. Hypothermia was produced by cannulating the femoral artery and vein and shunting the blood through a heat exchanger submerged in an ice water bath. Rewarming was accomplished by placing the heat exchanger in a warm water bath. Body temperature was measured by a thermistor-tipped catheter placed in the central venous system. Ouabain intoxication was produced by a single intravenous injection of ouabain, 0.084 mg/kg. Premature beats were induced by stimuli delivered to the ventricular driving sites with varying coupling intervals. Epinephrine was administered as an intravenous infusion of 2.0 μg/kg per minute.

When stimuli were applied only to the atrium, area maps included the P wave as well as the QRST. When atrium and ventricle were stimulated simultaneously, atrial excitation and recovery potentials were superimposed on those due to ventricular excitation. In the analysis to be described, maps based on deflection area during the control state were subtracted from maps recorded after interventions intended to alter vulnerability. Since atrial deflections were included in both control and test states, effects of atrial events were eliminated by the subtraction of maps.

Map Acquisition and Processing

All data were collected, using multiplexing hardware designed and developed in our laboratory for acquisition of body surface potential maps.[7] The multiplexing system consisted of six time division multiplexers, each of which amplified and switched 32 low level signals onto a single channel once every 1 msec. Each of the six multiplexer outputs was recorded on a single channel of a wide band FM instrumentation recorder at a speed of 120 inches per second (ips). A seventh tape channel was used to record a clock, synchronized to the multiplexers, and used for later demultiplexing of the data. The system effectively recorded 192 simultaneous ECGs with a 500-Hz bandwidth. A real time display of all 192 simultaneously recorded leads permitted verification that all ECG channels were operative. To eliminate ECG variation due to ventilation, the ventilator was held in expiration during the 10-second recording period. The recording system provided a flexible means of acquiring a great many maps over a short interval of time. Furthermore, the fact that data were recorded simultaneously permitted the acquisition of maps during rapidly changing cardiac states.

Recorded data were computer processed to yield scalar waveforms, isopotential maps, and isoarea maps. Data tapes were played back at 7.5 ips, digitized, and stored on digital magnetic tape. A single cardiac cycle was chosen for each run. Each of the 192 ECGs then was adjusted to baseline using linear interpolation between corresponding times of adjacent TP segments, and corrected for gain using a prerecorded calibration signal. In the event that a given lead was in error because of noise, electrode movement, or amplifier failure, potentials at that site were estimated, using an average of potentials at neighboring sites.

The resulting map data then were stored permanently on tape, filmed as isopotential maps on 16-mm film at 1- and 5-msec intervals during the QRS and T, respectively. Isoarea maps were calculated and plotted for QRS and T. An RMS voltage vs. time curve was plotted for each run. Onset of QRS, end of QRS, and end of T were selected manually. Due to the smoothing nature of the integrating process used to calculate area maps, slight differences in placement of these fiducial markers did not contribute significantly to the area maps. Areas of stimulus artifact obtained by integrating over its duration were found to be insignificant in comparison to changes observed in QRS, T, and QRST area maps due to the different experimental interventions. For the sake of consistency, stimulus artifacts were included in the area calculations for all premature beats and represented a small but constant error.

The control QRS and T area maps were determined for each dog prior to interventions known to alter vulnerability to arrhythmia. These maps were used to calculate a series of QRST area maps which were considered to be the control records for the vulnerability analysis.

Figure 1 illustrates the concept of the vulnerability analysis. A diagrammatic set of transmembrane action potentials and a single ECG lead are shown. Action potentials 1 and 2 are considered to represent adjacent cardiac areas, as are action potentials 2 and 3. Differences in the moment-by-moment time phase of phase 3 repolarization of action potentials 1 and 2 and of 2 and 3 are intended to represent the disparity of recovery between

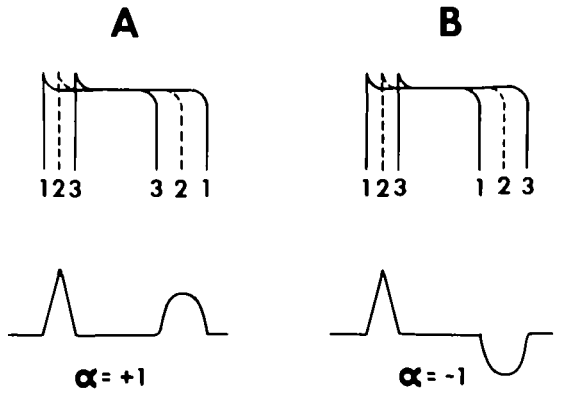

FIGURE 1 *Illustration of the concept of a nonvulnerable series of electrocardiographic waveforms. Diagrams of action potentials of nonuniform duration are shown. Panel A represents a normal control state in which the recovery sequence is opposite that of the activation sequence, and in panel B the recovery sequence is the same as the activation sequence. Although the two sets of action potentials would be associated with different waveforms, there is no greater disparity between action potentials labeled 1 and 2 or action potentials labeled 2 and 3 in panels A and B.*

these cardiac areas. The control state is illustrated in panel A. As shown in panel B, action potential durations can be altered to yield the inverse of the control recovery sequence without increasing the moment-by-moment disparity of recovery between areas 1 and 2 or between areas 2 and 3. A diagrammatic electrocardiogram associated with each of the action potential sets is also shown. The ECG shown in panel A represents the control QRS and T waveform. The T waveform and area shown in panel B are the inverse of the control T wave and reflect a change in action potential durations with reference to the control state. If the control state is considered to be normal, the conditions illustrated in panel B represent abnormal ventricular recovery. The abnormal recovery illustrated does not, however, include increased disparity of recovery between adjacent cardiac areas. The QRST areas illustrated in panels A and B differ, and it was hypothesized that all QRST areas between the extremes shown would reflect cardiac states in which the disparity of recovery did not exceed that in the control state. The concept illustrated in Figure 1 does not depend on the absolute duration of transmembrane action potentials. If the duration of action potentials in panel A were increased but the same relation of upstrokes and repolarization maintained, the duration of the QT interval would be increased with a longer isoelectric ST segment but the QRST area would remain the same.

For the purposes of this report, the term "disparity" of ventricular recovery will be used to indicate moment-by-moment differences in the degree of repolarization of various ventricular areas. If the entire ventricular mass repolarized simultaneously, no disparity of recovery would exist. Any other mode of recovery, including the normal, would exhibit disparity of recovery. The degree of disparity would vary with time and be determined by the voltage-time course of repolarization of the transmembrane action potential. The definition of disparity of recovery as varying with time is used in this report because the variation is one of the determinants of ST-T deflection waveform and area. We recognize that the principal evidence of a relation between the degree of disparity of recovery and vulnerability to arrhythmia has been obtained by measurements of refractory periods which establish only a single phase of recovery. It is likely, however, that greater than normal degrees of disparity also occur during other portions of the recovery process. The term "increased" disparity of recovery will be used to indicate greater degrees of disparity than exist in normal or control states. The term "local" disparity of recovery as used in this report requires explanation. The relation of disparate recovery and vulnerability has been established by refractory period measurements in localized cardiac areas. Within such areas, the range of refractory periods has been shown to be increased by interventions which enhance vulnerability to arrhythmia. These include local lesions such as ischemia and interventions which affect the entire cardiac mass, such as ouabain intoxication and hypothermia. For the purposes of this report, the term "increased local" disparity of recovery will be used to indicate conditions of greater than normal or control degrees of recovery disparity at cardiac sites in close proximity to each other, whether these conditions exist in a local area only or in the entire ventricle.

The concept illustrated in Figure 1 for a single electrocardiographic lead was applied to the body surface pattern of QRST areas sampled with 192 leads. The control QRST area pattern was taken as one extreme of the hypothetical series. Other maps in the series consisted of the control QRS area map plus various fractions of the control T area map to the extreme of −100% of the T area map. Map patterns in this series were regarded as ones which could occur without increased local disparity of recovery times and without increased vulnerability to arrhythmia on that basis. The control QRST isoarea map and those calculated from it will be referred to as the "nonvulnerable" map series.

QRST isoarea maps after interventions known to alter vulnerability to arrhythmia (test maps) were compared to those in the nonvulnerable series, and the "best match" was determined. In that determination, the QRST area in each lead of the test map was compared to that of the same lead in maps from the nonvulnerable series. The best match was taken as that map from the series with the smallest total QRST area difference from all leads of the test map. Finally, the difference between the test map and its best match from the nonvulnerable series was determined and displayed as a map that was titled the "vulnerability map." The following equations were used to calculate the vulnerability map:

$$tAQRST - (cAQRS + \alpha \cdot cAT) = V \qquad (1)$$

where α is determined by minimizing squared differences.

$$\frac{d}{d\alpha}[tAQRST - (cAQRS + \alpha \cdot cAT)]^2 = 0$$

$$\alpha = \frac{tAQRST \cdot cAT - cAQRS \cdot cAT}{cAT \cdot cAT} \qquad (2)$$

where:

tAQRST = QRST area of the test map
cAQRS = QRS area of the control map
cAT = T area of the control map
V = vulnerability map
α = the fraction of the control T area combined with the control QRS area to yield a QRST area map in the non vulnerable series.

A vulnerability index with units of mV·msec was calculated by taking the square root of the sum of the squares of the 192 values contained in the vulnerability map. The meaning of the vulnerability map and index can be illustrated by considering the case in which the control QRST isoarea map assumes the role of the test state. In this case, the vulnerability map would contain all zeros, and the vulnerability index would be zero.

Results

Figure 2 is an example of control isoarea maps from one experiment. The QRS isoarea map is shown in panel A and the T isoarea map in panel B. Panel C shows the QRST isoarea map and panel D the QRS-T isoarea map which represent the extremes of the "nonvulnerable" QRST isoarea map series for this dog. As described above, vulnerability maps were calculated by selecting the map from the "nonvulnerable" series showing the smallest difference from a test QRST isoarea map and subtracting it from the test QRST isoarea map.

In three dogs, vulnerability maps and indices were obtained at 2-minute intervals following a single intravenous injection of ouabain, 0.084 mg/kg. Heart rate control was maintained by catheter electrode drive of the right ventricle. Figure 3 shows a plot of the vulnerability index as a function of time for these dogs. In one dog, the vulnerability index showed a monotonic increase with time from 4 to 40 minutes after injection. In this dog, spontaneous ventricular fibrillation occurred 1 minute after the 40-minute record. The increase in vulnerability index with time also was evident in the other two dogs, but fewer records were obtained because of loss of heart rate control. Also displayed on this plot is the $P < 0.001$ confidence limits of the beat-to-beat variation in vulnerability index. This value was calculated from 10 successive QRST areas from five experiments. These confidence limits indicated that the increase in vulnerability index with ouabain could not be explained by beat-to-beat physiological variation.

Examples of the QRST isoarea maps and their best match from the nonvulnerable QRST isoarea map series are shown in Figure 4. The examples are from one of the experiments illustrated by vulnerability indices in Figure 3. Panel A shows the QRST isoarea map 4 minutes after injection of ouabain and panel B the best match for this map from the nonvulnerable series. It is apparent that major features of the maps are similar and subtraction could be expected to yield a small difference. Panel C of

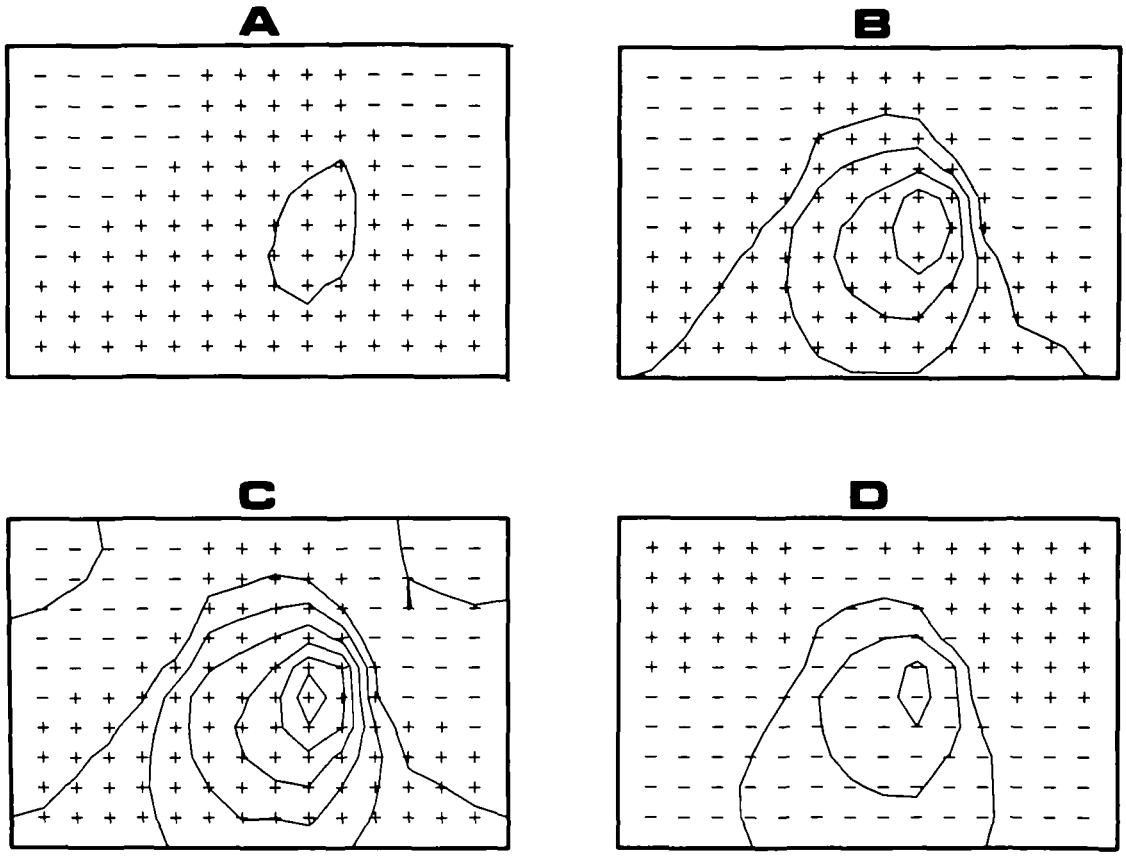

FIGURE 2 *Isoarea maps of the QRS (A), T (B), QRST (C), and QRS-T (D) of one dog. The QRST and QRS-T isoarea maps represent the extremes of the nonvulnerable series of maps. Contour lines are drawn at intervals of 40 mV·msec.*

Figure 4 shows the QRST isoarea map 40 minutes after ouabain injection, and panel D shows the best match for this map from the calculated nonvulnerable series. There are gross differences between the QRST isoarea map and its best match from the nonvulnerable series, and subtraction would be expected to show a large difference. Figure 5 shows the vulnerability maps from the experiment illustrated in Figure 4. These maps showed an increasing density of contour lines with increasing time following injection of ouabain. Sequential vulnerability maps from the other two dogs showed similar patterns and time course.

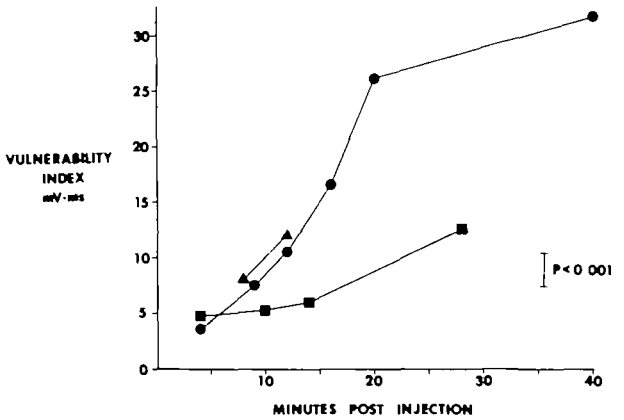

FIGURE 3 *Graph of increase in vulnerability index following iv injection of ouabain, 0.84 mg/kg, in three dogs. The confidence limits at the $P < 0.001$ level calculated from 10 successive complexes in five experiments are shown in the lower righthand corner.*

In three dogs, states of enhanced vulnerability were produced by premature depolarizations initiated by stimuli delivered simultaneously to atria and ventricles. The isoarea map of a single premature beat was determined by subtracting the QRST isoarea map during regular basic drive from one including the areas of both the premature complex and preceding basic drive complex. The QRST isoarea map of the second of two premature beats was obtained by subtracting the map of a combined basic drive and a single premature complex from a map including the area of a basic drive complex and both premature complexes. In these dogs, basic driving stimuli with a cycle length of 400 msec and premature stimuli were delivered to the same ventricular sites. Figure 6 shows the vulnerability maps of three premature beats with varying coupling intervals. The premature stimuli were delivered 300 msec after the basic drive in map A, 250 msec after the basic drive in map B, and 200 msec after the basic drive in map C. The amplitude of the vulnerability maps increased with increasing prematurity

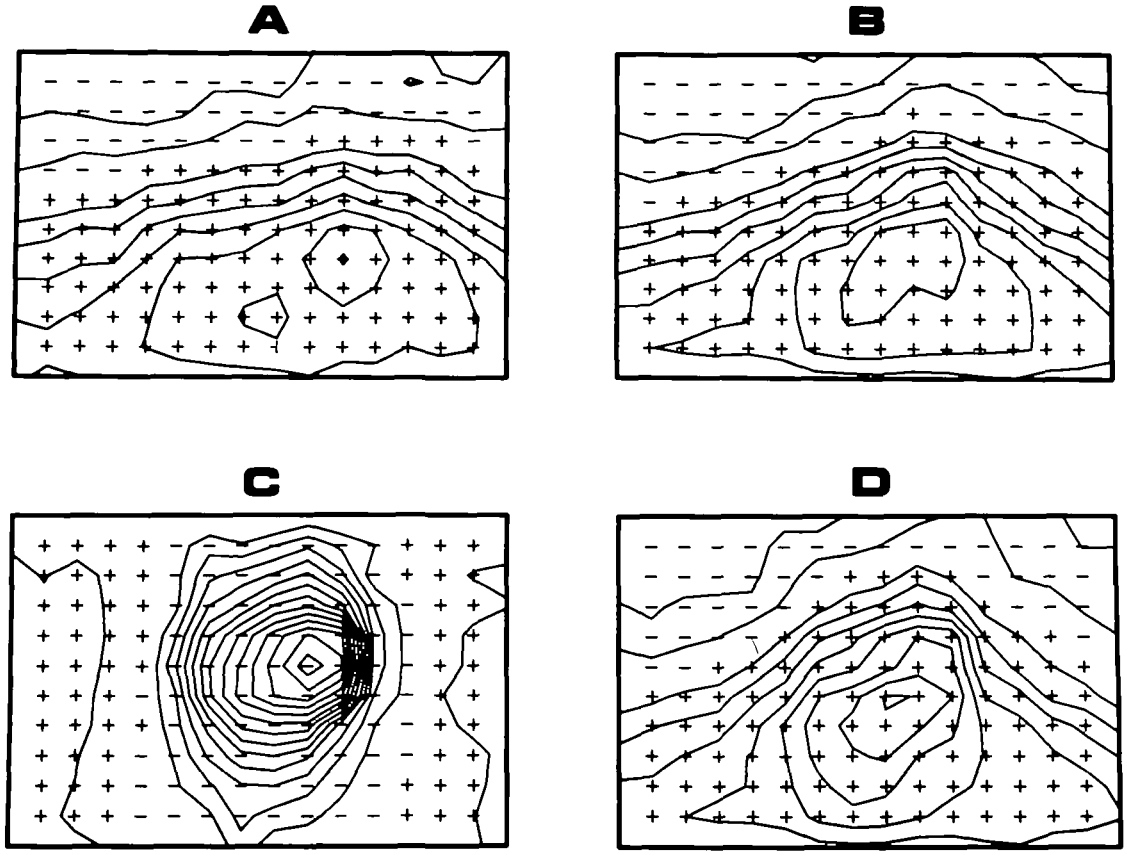

FIGURE 4 *Examples of QRST area maps of one dog and their "best match" from the nonvulnerable map series. Panel A shows the QRST area map of a dog 4 minutes after the injection of a toxic dose of ouabain; panel B shows the best match of that map from the nonvulnerable map series. Panel C shows the QRST area map 40 minutes after ouabain injection. The best match map from the nonvulnerable series is shown in panel D.*

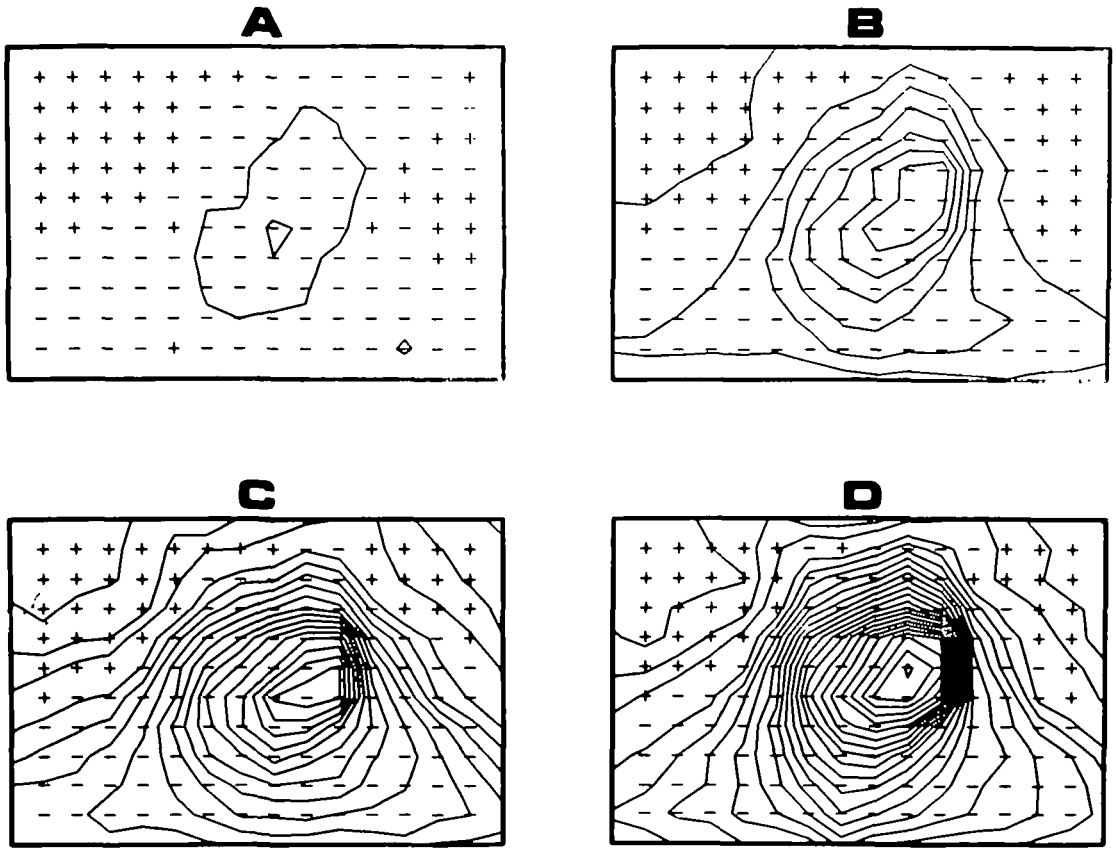

FIGURE 5 *Vulnerability maps showing progressively increasing density at 4 minutes (A), 12 minutes (B), 20 minutes (C), and 40 minutes (D) after ouabain injection in one dog. Contour lines are drawn at 20-mv·msec intervals. Spontaneous ventricular fibrillation occurred at 41 minutes postinjection.*

of the stimuli. Increasing prematurity of stimuli to a right ventricular site and to a combination of right and left ventricular sites in this dog showed a similar increase in the density of contour lines in the vulnerability maps. Similar results were obtained for the other two dogs. An example of the vulnerability maps during the first and second of two premature beats is shown in Figure 7. The first map was taken following a premature stimulus delivered to the left ventricle and delayed by 300 msec from a basic drive with a 400-msec cycle length. The second map was of a premature beat with a cycle length of 160 msec after the 300-msec premature beat. The density of the vulnerability map was greater for the second of two premature beats than the first. Similar results were obtained with successive premature beats in the other two dogs.

Hypothermia and rewarming were performed in experiments on two dogs. Heart rate control was maintained by catheter electrode drive of the left ventricle. Figure 8 is a plot of the vulnerability index as a function of temperature of a dog that was cooled to 27°C and rewarmed. The vulnerability index increased during cooling and returned to control values following rewarming with a slight increase in the index at the beginning of rewarming. A similar pattern of the vulnerability index was observed during other episodes of cooling and rewarming in this and the other dog.

An infusion of epinephrine, 2.0 μg/kg per minute, was administered intravenously in two dogs. A constant heart rate was maintained by catheter electrode drive of the right atrium. Figure 9 displays the changes of the vulnerability index during a 10-minute infusion in one dog. During the first 3 minutes of infusion, the vulnerability index was high. This corresponded to the period of increased disparity of recovery of excitability previously reported by Han et al.[4] and attributed to the initial inhomogeneous distribution of the drug to the myocardium. Following this initial period, the vulnerability index remained at near zero values while the infusion was continued and after it was terminated. A similar pattern of changes in the vulnerability index was observed in the other dog.

Discussion

Our findings in this study suggest that conditions of increased local disparity of ventricular recovery which increase vulnerability to arrhythmia can be detected by analysis of the body surface electrocardiogram. Detection requires leads with sensitivity selective to various cardiac areas, since the established relation of vulnerability to arrhythmia and ventricular recovery is that of disparate recovery in localized areas. In this study, ECGs recorded from 192 electrodes on dogs were used, but evidence has been reported that considerably fewer electrodes are

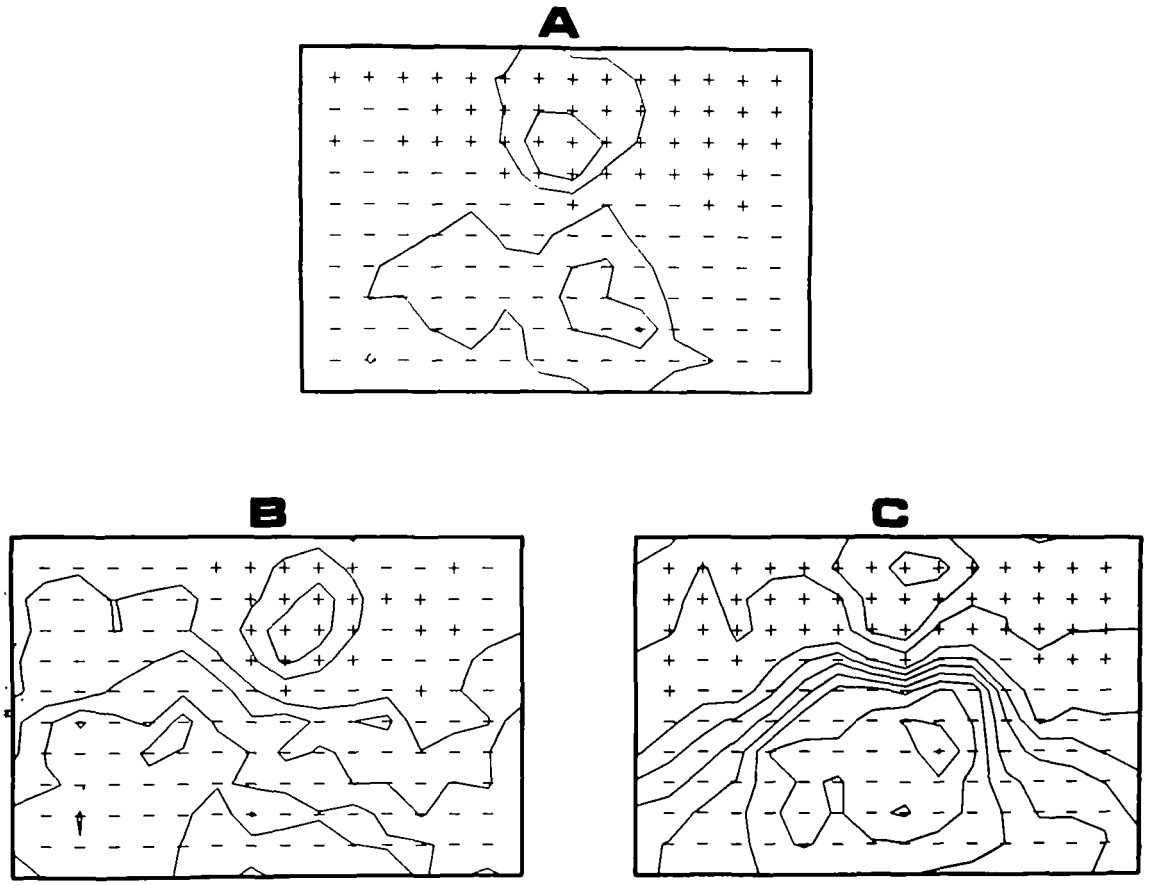

FIGURE 6 *Vulnerability maps of single premature depolarizations induced with stimuli delivered to the left ventricle with 300-msec (A), 250-msec (B), and 200-msec (C) coupling intervals following basic cycle lengths of 400 msec. Contour lines are drawn at 20-mv·msec intervals. The maps show increased density with increasing prematurity of complexes.*

required for regional cardiac examination in humans.[8, 9] Lead systems using 24 and 32 electrodes at selected sites have been reported to furnish up to 99% of the information contained in the body surface potential patterns determined with 150–192 electrodes. Use of the smaller number of electrodes for body surface potential mapping would facilitate not only electrode placement but also the simultaneous acquisition of data from all electrodes.

The electrocardiographic detection of disparate recovery related to vulnerability to arrhythmia also must take into account the possibility that abnormal recovery properties and the resulting abnormal T waves do not necessarily involve abnormal local disparity of recovery. This possibility was recognized in our study by calculating a hypothetical series of "nonvulnerable" QRST area maps. The series included abnormal T waves attributable to abnormal recovery properties but without abnormal regional disparity of recovery times.

Detection of locally disparate recovery affecting vulnerability to arrhythmia also requires an electrocardiographic index that is not substantially affected by activation sequence. Abnormalities of the T wave, secondary to changes in activation order only, are not likely to result in locally disparate recovery. Normal ventricular excitation begins near the center of the cardiac mass and proceeds in multiple directions simultaneously. Abnormal activation such as that occurring during ventricular ectopic beats proceeds from the site of origin, which may be eccentric, requires a longer time for completion, and causes prolongation of the QRS complex. The abnormal activation sequence affects the recovery sequence and results in secondary changes of the ST-T deflection. The abnormal recovery sequence probably involves increased disparity of earliest and latest recovery times in the entire ventricular mass, but, within local areas, the time required for excitation and the degree of disparity of recovery times are not necessarily affected. The QRST area of the electrocardiogram fulfills the requirement of being largely independent of activation sequence. Small differences of this quantity associated with varied activation orders probably are the result of varied electrotonic interactions during repolarization and thus reflect actual differences of ventricular recovery properties which should be included in the detection of local disparity of recovery.[6]

Limitations of the proposed method of assessing vulnerability include all those inherent in a regional cardiac examination by means of the electrocardiogram. For example, differences in the sensitivity of body surface leads to various cardiac regions have been demonstrated in previous studies.[10] It is therefore unlikely that equal degrees of abnormally disparate recovery in different cardiac areas will have equal effects on estimates of

vulnerability. It is likely that some conditions of increased disparity of recovery cannot be detected by electrocardiographic means. Signals resulting from these conditions are subject to cancellation because of opposing directions of recovery, as are other electrocardiographic events. Application of estimates of vulnerability to humans will add other limitations. In this study, the record from a given dog prior to a particular intervention was considered to be the control and was compared to records obtained after vulnerability to arrhythmia had been altered. Use of the method to study humans will require a different standard, such as the average normal QRS and T isoarea maps. The range of normal variation also will have to be considered and undoubtedly will limit the method's sensitivity and specificity. It also should be recognized that this study does not constitute proof that cardiac conditions responsible for vulnerability to arrhythmia also were responsible for the electrocardiographic findings reported. It is possible that altered vulnerability and the ECG findings were independent effects of the various interventions. This seems unlikely in view of the previously demonstrated relation of disparate recovery to vulnerability to arrhythmia and the fact that the ECG analysis used in this study was specifically designed to detect disparate recovery. It also seems unlikely since the vulnerability index was increased by multiple interventions with different effects on recovery properties but all known to alter vulnerability. More direct proof that results of the ECG analysis are directly due to cardiac conditions responsible

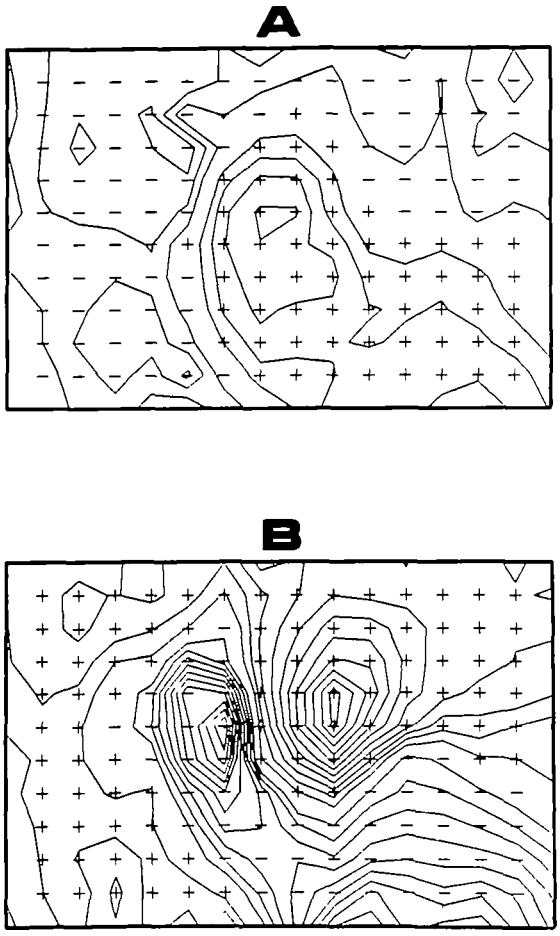

FIGURE 7 *Panel A shows the vulnerability map of a single premature depolarization at 300 msec during basic drive with a cycle length of 400 msec. Panel B shows the vulnerability map of a second premature depolarization at 160 msec following the 300-msec premature depolarization. Both basic and premature stimuli were delivered to the left ventricle. Contour lines were drawn at 20-mv·msec intervals. The maps show increased density with the second early premature beat.*

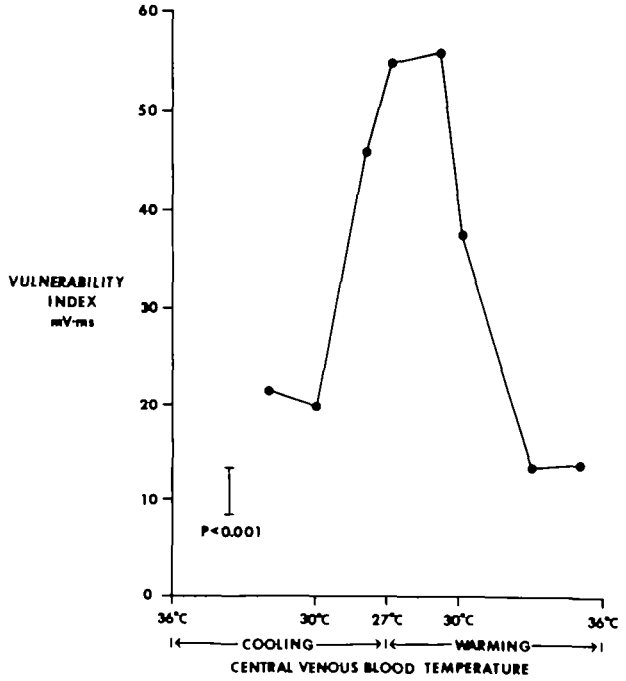

FIGURE 8 *The graph showing changes in vulnerability index during hypothermia and rewarming in one dog. The confidence limits as shown in Figure 3 are indicated in the lower lefthand corner.*

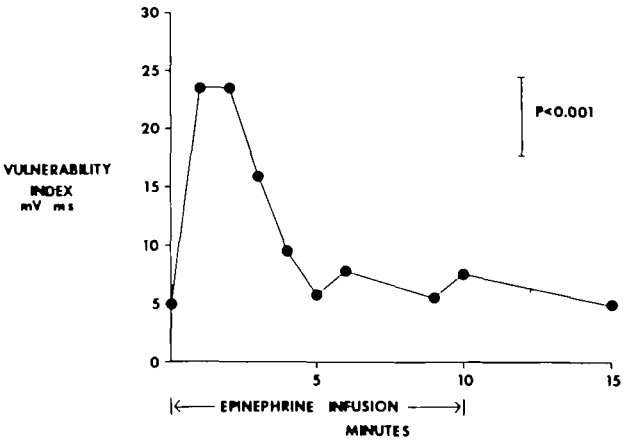

FIGURE 9 *Graph showing changes in vulnerability index during and following a 10-minute iv infusion of epinephrine, 2.0 μg/kg per minute. Within 1 minute of infusion, the vulnerability index increased but returned to near control values after 5 minutes. The confidence limits, as shown in a previous figure, are indicated in the upper righthand corner.*

for altered vulnerability to arrhythmia is, nevertheless, desirable.

Although both the mechanisms involved and the utility of the method reported require further evaluation, this study suggests enhanced vulnerability to arrhythmia, when due to disparate ventricular recovery, can be detected by appropriate analysis of the body surface electrocardiogram.

References

1. Han J, Moe GK: Nonuniform recovery of excitability in ventricular muscle. Circulation **14:** 44-60, 1964
2. Han J, Garcia de Jalon PD, Moe GK: Adrenergic effects on ventricular vulnerability. Circ Res **14:** 516-524, 1964
3. Han J, Garcia de Jalon PD, Moe GK: Fibrillation threshold of premature ventricular responses. Circ Res **18:** 18-25, 1966
4. Han J, Millet D, Chizzonittu B, Moe GK: Temporal dispersion of recovery of excitability in atrium and ventricle as a function of heart rate. Am Heart J **71:** 481-487, 1966
5. Harumi K, Burgess MJ, Abildskov JA: A theoretic model of the T wave. Circulation **34:** 657-668, 1966
6. Abildskov JA, Burgess MJ, Urie PM, Lux RL, Wyatt RF: The unidentified information content of the electrocardiogram. Circ Res **40:** 3-7, 1977
7. Wyatt RF, Lux RL: Application of multiplexing techniques in the collection of body surface maps from single complexes. *In* Advances in Cardiology, vol 10, edited by S Rush, E Lepeschkin. Basel, S. Karger, 1974, pp 26-32
8. Lux RL, Smith CR: Optimal sequential lead selection in body surface potential mapping (abstr). Proceedings of the 28th Annual Conference on Engineering in Medicine and Biology. **17:** 56, 1975
9. Barr RC, Spach MS, Herman-Giddens GS: Selection of the number and positions of measuring locations for electrocardiography. IEEE Trans Biomed Eng **18:** 125-138, 1971
10. Abildskov JA, Burgess MJ, Lux RL, Wyatt RF: Experimental evidence for regional cardiac influence in body surface isopotential maps of dogs. Circ Res **38:** 386-391, 1976

Adenosine Metabolism in Canine Myocardial Reactive Hyperemia

R. A. OLSSON, J. A. SNOW, AND M. K. GENTRY

SUMMARY **In pentobrabital-anesthetized open-chest dogs, myocardial adenosine content is elevated by 5 or 15 seconds of left coronary artery occlusion and falls exponentially to control levels during reactive hyperemia. The rate constants for adenosine dissipation are (mean ± SEM): -0.08 ± 0.01 and -0.034 ± 0.007 sec^{-1} after 5- and 15-second occlusion, respectively. Kinetic analysis of the reactive hyperemia flow curves (Circ Res 14/15 (suppl I): 81-85, 1963) predicts rates of -0.069 ± 0.009 sec^{-1} and -0.04 ± 0.009 sec^{-1}, indicating that changes in adenosine levels can account for the way coronary flow changes during this response. The log (dose-) response curve relating reactive hyperemia flow to tissue adenosine concentration has a steeper slope and is half-maximal at a lower adenosine concentration than the dose-response curve obtained by intracoronary infusions of adenosine in oxygenated hearts, indicating that the coronary vasoactivity of adenosine is enhanced during reactive hyperemia. This could explain why theophylline antagonizes the coronary vasodilatory effect of adenosine in oxygenated hearts but has relatively little effect on reactive hyperemia.**

ADENOSINE has been detected in coronary venous blood during myocardial reactive hyperemia, a finding which has been interpreted as evidence that this nucleoside may regulate coronary vascular tone during the hyperemia response.[1] In support of this, adenosine has been demonstrated in oxygenated heart muscle, the amount found increasing rapidly during myocardial ischemia.[2, 3] However, the adenosine content of heart muscle and coronary venous blood have not been related to coronary blood flow rate during reactive hyperemia, so that these findings must be considered as only circumstantial support for the adenosine hypothesis. Indeed, reports that doses of aminophylline which strongly antagonize the coronary vasodilation caused by adenosine have a disproportionately smaller effect on myocardial reactive hyperemia[4-7] suggest that adenosine may have no role at all in the hyperemia response.

The studies reported herein examine two questions. (1) How do cardiac adenosine levels change with time during myocardial reactive hyperemia? (2) Is the relationship betweeen cardiac adenosine levels and coronary flow during postischemic reactive hyperemia the same as it is during an intracoronary infusion of this nucleoside in an oxygenated heart?

The experiments designed to answer the first question were based on a preliminary study from this laboratory[8] which showed that if one assumes that coronary blood flow rate during myocardial reactive hyperemia is regulated by a vasodilatory metabolite which accumulates during ischemia and that the log (dose-) response approximation describes the relationship between flow and the concentration of this metabolite, the metabolite should have the following properties: (1) it is present in oxygenated as well as ischemic heart muscle; (2) it accumulates

From the Department of Cardiorespiratory Diseases, Walter Reed Army Institute of Research, Washington, D.C.

Dr. R. A. Olsson's present address (and address for reprints) is: Department of Internal Medicine, University of South Florida College of Medicine, Tampa, Florida 33620.

Received June 6, 1977; accepted for publication October 11, 1977